arXiv:cond-mat/0405310v1 [cond-mat.supr-con] 14 May 2004

The effects of Zn Impurity on the Properties of Doped Cuprates in the Normal State

Yun Song
Department of Physics, Beijing Normal University, Beijing 100875, China
(March 22, 2022)

We study the interplay of quantum impurity, and collective spinon and holon dynamics in Zn doped high-T_c cuprates in the normal state. The two-dimensional t-t′-J models with one and a small amount of Zn impurity are investigated within a numerical method based on the double-time Green function theory. We study the inhomogeneities of holon density and antiferromagnetic correlation background in cases with different Zn concentrations, and obtain that doped holes tend to assemble around the Zn impurity with their mobility being reduced. Therefore a bound state of holon is formed around the nonmagnetic Zn impurity with the effect helping Zn to introduce local antiferromagnetism around itself. The incommensurate peaks we obtained in the spin structure factor indicate that Zn impurities have effects on mixing the q=(π, π) and q=0 components in spin excitations.

75.30.Hx, 74.72.-h, 74.20.Mn

The effects of divalent transition metal Zn substitute for Cu in CuO_2 plane present much valuable information in understanding the mechanism of high temperature superconductors. Zn^{2+} has a closed d shell with spin $s = 0$, and acts as a very strong scattering center. As a result, the spin configurations and the electronic structures around the nonmagnetic impurity Zn are strongly disrupted in both the normal state and superconducting state. Below T_c, there have been many experimental [1–5] and theoretical [6–10] investigations to discover how the d-wave superconductivity is destroyed and what is the microscopic mechanism behind. As the normal state properties are more fundamental, some experimental [11–15] and theoretical [16–18] works have been done to study the effects of nonmagnetic impurity Zn on the properties of normal state. It is believed that these studies are of great help for understanding the peculiar behaviors of normal state. Moreover, they shed light on the recent striking issue of the normal state pseudogap [19,20]. So far, there has been no clear picture of how the impurity interplays with the strong correlation background. It still remains unanswered why the Zn impurity produced very strong scatter and how the impurity band forms in real space.

In this paper, we perform numerical calculation to study the effects of Zn impurity on its surrounded Cu ions in the normal state. We want to find out how the Zn impurity influences the hole distribution and AF correlation background, which may bring about a better understanding of the fundamental relation between spin and hole. We start from the two-dimensional (2D) t-t′-J model and use fermion-spin theory [21]. Fermion-spin theory is based on the charge-spin separation, in which the single occupied constrain of t-t′-J model could be treated properly even in the mean field approximation. Within an improved Green function theory [22], we perform numerical calculation for cases with only one Zn impurity and a small amount of Zn impurity, and the effect of Zn concentration on some properties of the normal state are discussed.

The essential physics of high-T_c cuprates is well described by the t-J model on a square lattice. In the condition that Zn substitutes Cu in CuO_2 plane, we can model Zn impurity as vacant site, which has no coupling with surrounded Cu sites. We add the next-nearest-neighbor hopping term in our model to reproduce the realistic band structure, and start our study from the following Hamiltonian

$$H = -t \sum_{\langle i,j\rangle \neq l,\sigma} (C^{\dagger}_{i\sigma} C_{j\sigma} + h.c.) - t' \sum_{\langle i,i'\rangle \neq l,\sigma} (C^{\dagger}_{i\sigma} C_{i'\sigma} + h.c.) - \mu \sum_{i,\sigma} C^{\dagger}_{i\sigma} C_{i\sigma} + J \sum_{\langle i,j\rangle \neq l} \mathbf{S_i} \cdot \mathbf{S_j}, \quad (1)$$

where $\langle i,j\rangle$ and $\langle i,i'\rangle$ mean the summations over nearest-neighbor (NN) and next-nearest-neighbor (NNN) pairs respectively, and l represents the site occupied by Zn impurity. In our model the direct hopping among a Zn impurity and its surrounded Cu sites is forbidden. In addition, to eliminate the doubly occupied sites of Cu ion, we introduce constraint $\sum_\sigma C^{\dagger}_{i\sigma} C_{i\sigma} \leq 1$ for each Cu site. Also we introduce $\sum_\sigma C^{\dagger}_{l\sigma} C_{l\sigma} = 2$ for Zn^{2+} ion since it has a closed d shell. Therefore, the total number of electrons satisfies $\sum_{i\sigma} C^{\dagger}_{i\sigma} C_{i\sigma} = N - N_h + N_{Zn}$ with N_h and N_{Zn} representing the number of hole and Zn impurity, respectively. As the strong electron correlation manifests itself by the local constraint, the key issue is how to treat the constraint properly.

Here we study the t-t′-J model within the fermion-spin theory [21] based on the charge-spin separation. We introduce $C_{i\uparrow} = h^{\dagger}_i S^{-}_i$ and $C_{i\downarrow} = h^{\dagger}_i S^{+}_i$, where the spinless fermion operator h_i describes the charge (holon) degrees of freedom, while the pseudospin operator S_i describes the spin (spinon) degrees of freedom. Thus the low energy behavior of the t-t′-J model (1) can be written as

$$H = -t \sum_{\langle i,j\rangle \neq l} (h_i h^{\dagger}_j + h_j h^{\dagger}_i)(S^{+}_i S^{-}_j + S^{-}_i S^{+}_j)$$

$$-t'\sum_{\langle i,i'\rangle\neq l}(h_i h_{i'}^\dagger + h_{i'}h_i^\dagger)(S_i^+S_{i'}^- + S_i^-S_{i'}^+)$$
$$+\mu\sum_{i\neq l}h_i^\dagger h_i + \sum_{\langle i,j\rangle\neq l}J_{i,j}^{\rm eff}\mathbf{S}_i\cdot\mathbf{S}_j, \quad (2)$$

where $J_{i,j}^{\rm eff}=[(1-n_i^h)(1-n_j^h)-\phi_{i,j}^2]J$ with n_i^h representing the hole concentration at site i and $\phi_{i,j}=\langle h_i^\dagger h_j\rangle$ being the order parameter of holon. Here we also introduce spinon correlation functions $\chi_{ij}=\langle S_i^-S_j^+\rangle$ and $\chi_{ij}^z=\langle S_i^zS_j^z\rangle$.

We introduce three double-time Green functions

$$\begin{aligned}G_h(i-j,\ \tau-\tau') &= -i\theta(\tau-\tau')\langle[h_i(\tau),\ h_j^+(\tau')]\rangle\\ &\equiv\langle\langle h_i(\tau);h_j^+(\tau')\rangle\rangle\\ D_s(i-j,\ \tau-\tau') &= -i\theta(\tau-\tau')\langle[S_i^+,\ S_j^-(\tau')]\rangle\\ &\equiv\langle\langle S_i^+(\tau);S_j^-(\tau')\rangle\rangle\\ D_s^z(i-j,\ \tau-\tau') &= -i\theta(\tau-\tau')\langle[S_i^z,\ S_j^z(\tau')]\rangle\\ &\equiv\langle\langle S_i^z(\tau);S_j^z(\tau')\rangle\rangle, \quad (3)\end{aligned}$$

where G_h describes the behaviors of holon, and D_s and D_s^z describe the behaviors of spinon. Since the lattice translational invariance is not presented in cases with Zn impurities, we evaluate the equations of motion of the above Green's functions in real space. The double-time Green function $\langle\langle A;\ B\rangle\rangle$ satisfies

$$\omega\langle\langle A;\ B\rangle\rangle_\omega = \langle[A,\ B]_\mp\rangle_\omega + \langle\langle[A,\ H];\ B\rangle\rangle_\omega, \quad (4)$$

thus we could obtain the equations of motion of G_h

$$(\omega-\mu)G_h(i-j)_\omega - 2t\sum_\eta\chi_{i,i+\eta}G_h(i+\eta-j)_\omega$$
$$-2t'\sum_\tau\chi_{i,i+\tau}G_h(i+\tau-j)_\omega=\delta(i-j). \quad (5)$$

We introduce $\widetilde{G}_h$, a $N^2\times N^2$ elements matrix, to express the holon Green functions for a square lattice with $N\times N$ sites. And we could rewrite Eq. (5) as

$$(\omega-\mu)\widetilde{G_h} - \widetilde{h}\ \widetilde{G_h} = \widetilde{I}, \quad (6)$$

where matrix $\widetilde{h}$ is decided by the NN and NNN spinon correlation functions, and $\widetilde{I}$ is an identity matrix.

Based on Eq. (3) and (4), we also obtain the equations of motion of spinon Green functions D_s and D_s^z

$$\begin{aligned}\omega D_s(i-j)_\omega &= 2\sum_\eta J_{i,i+\eta}^{eff}\{\epsilon_{i,i+\eta}F_1(i,i+\eta;\ j)_\omega\\ &\quad -F_1(i+\eta,i;\ j)_\omega\}\\ &\quad +8t'\sum_\tau\phi_{i,i+\tau}F_1(i,i+\tau;\ j)_\omega\\ \omega D_s^z(i-j)_\omega &= \sum_\eta J_{i,i+\eta}^{eff}\epsilon_{i,i+\eta}\{F_2(i,i+\eta;\ j)_\omega\\ &\quad -F_2(i+\eta,i;\ j)_\omega\}\\ &\quad +4t'\sum_\tau\phi_{i,i+\tau}\{F_2(i,i+\tau;\ j)_\omega\\ &\quad -F_2(i+\tau,i;\ j)_\omega\}, \quad (7)\end{aligned}$$

where $\epsilon_{i,i+\eta}=1+\frac{4t\phi_{i,i+\eta}}{J_{i,i+\eta}^{eff}}$. F_1 and F_2 are the second-order spinon Green functions which are defined as

$$\begin{aligned}F_1(i,l;\ j)_\omega &= \langle\langle S_i^zS_l^+;\ S_j^-\rangle\rangle_\omega\\ F_2(i,l;\ j)_\omega &= \langle\langle S_i^+S_l^-;\ S_j^z\rangle\rangle_\omega. \quad (8)\end{aligned}$$

Going a step further, we establish the equations of motion of the second-order spinon Green functions

$$\begin{aligned}\omega F_1(i,l;\ j)_\omega &= 2\chi_{i,l}^z\delta(l-j)-\chi_{i,l}\delta(i-j)\\ &\quad +\langle\langle\{\sum_\eta[2J_{l,l+\eta}^{eff}(\epsilon_{l,l+\eta}S_i^zS_l^zS_{l+\eta}^+ - S_i^zS_{l+\eta}^zS_l^+)\\ &\quad +J_{i,i+\eta}^{eff}\epsilon_{i,i+\eta}(S_i^+S_{i+\eta}^-S_l^+ - S_{i+\eta}^+S_i^-S_l^+)]\\ &\quad +4t'\sum_\tau[\phi_{i,i+\tau}(S_i^+S_{i+\tau}^-S_l^+ - S_{i+\tau}^+S_i^-S_l^+)\\ &\quad +2\phi_{l,l+\tau}S_i^zS_l^zS_{l+\tau}^+]\};S_j^-\rangle\rangle_\omega\\ \omega F_2(i,l;\ j)_\omega &= \chi_{i,l}\delta(l-j)-\chi_{i,l}\delta(i-j)\\ &\quad +\langle\langle\{\sum_\eta[2J_{l,l+\eta}^{eff}(S_i^+S_l^-S_{l+\eta}^z - \epsilon_{l,l+\eta}S_i^+S_{l+\eta}^-S_l^z)\\ &\quad +2J_{i,i+\eta}^{eff}(\epsilon_{i,i+\eta}S_{i+\eta}^+S_l^-S_i^z - S_i^+S_l^-S_{i+\eta}^z)]\\ &\quad +8t'\sum_\tau[\phi_{i,i+\tau}S_{i+\tau}^+S_l^-S_i^z\\ &\quad -\phi_{l,l+\tau}S_i^+S_{l+\tau}^-S_l^z]\};\ S_j^z\rangle\rangle_\omega. \quad (9)\end{aligned}$$

To the third-order spinon Green functions in the right hand side of Eq. (9), we perform the improved decoupling scheme as described in Ref. 22, for example

$$\langle\langle S_i^zS_l^zS_{l+\eta}^+;\ S_j^-\rangle\rangle\to\alpha_i\langle S_i^zS_l^z\rangle\alpha_l\langle\langle S_{l+\eta}^+;\ S_j^-\rangle\rangle. \quad (10)$$

Therefore, the second-order spinon Green functions F_1 and F_2 can be expressed by the Green functions D_s and D_s^z as

$$\begin{aligned}\omega F_1(i,l;\ j)_\omega &= \Gamma_1^0+\Gamma_1^1D(i-j)+\Gamma_1^4D(l-j)\\ &\quad +\sum_\eta\{\Gamma_1^2D(i+\eta-j)+\Gamma_1^3D(l+\eta-j)\}\\ &\quad +\sum_\tau\{\Gamma_1^5D(i+\tau-j)+\Gamma_1^6D(l+\tau-j)\}\\ \omega F_2(i,l;\ j)_\omega &= \Gamma_2^0+\Gamma_2^1D^z(i-j)+\Gamma_2^4D^z(l-j)\\ &\quad +\sum_\eta\{\Gamma_2^2D^z(i+\eta-j)+\Gamma_2^3D^z(l+\eta-j)\},\end{aligned} \quad (11)$$

where

$$\begin{aligned}\Gamma_1^0 &= 2\chi_{i,l}^z\delta(l-j)-\chi_{i,l}\delta(i-j)\\ \Gamma_1^1 &= \sum_\eta J_{i,i+\eta}^{eff}\epsilon_{i,i+\eta}\alpha_{i+\eta}\chi_{i+\eta,l}\alpha_l\\ &\quad +4t'\sum_\tau\phi_{i,i+\tau}\alpha_{i+\tau}\chi_{i+\tau,l}\alpha_l\\ \Gamma_1^2 &= -J_{i,i+\eta}^{eff}\epsilon_{i,i+\eta}\alpha_i\chi_{i,l}\alpha_l\end{aligned}$$

$$
\begin{aligned}
\Gamma_1^3 &= 2J_{l,l+\eta}^{eff}\epsilon_{l,l+\eta}\alpha_i\chi_{i,l}^z\alpha_l \\
\Gamma_1^4 &= -2\sum_\eta J_{l,l+\eta}^{eff}\alpha_i\chi_{i,l+\eta}^z\alpha_{l+\eta} \\
\Gamma_1^5 &= -4t'\phi_{i,i+\tau}\alpha_i\chi_{i,l}\alpha_l \\
\Gamma_1^6 &= 8t'\phi_{l,l+\tau}\alpha_i\chi_{i,l}^z\alpha_l \\
\Gamma_2^0 &= \chi_{i,l}\delta(l-j) - \chi_{i,l}\delta(i-j) \\
\Gamma_2^1 &= 2\sum_\eta J_{i,i+\eta}^{eff}\epsilon_{i,i+\eta}\beta_{i+\eta}\chi_{i+\eta,l}\beta_l \\
&\quad +8t'\sum_\tau \phi_{i,i+\tau}\beta_{i+\tau}\chi_{i+\tau,l}\beta_l \\
\Gamma_2^2 &= -2J_{i,i+\eta}^{eff}\beta_i\chi_{i,l}\beta_l \\
\Gamma_2^3 &= 2J_{l,l+\eta}^{eff}\beta_i\chi_{i,l}\beta_l
\end{aligned}
\tag{12}
$$

and

$$
\begin{aligned}
\Gamma_2^4 = &-2\sum_\eta J_{l,l+\eta}^{eff}\epsilon_{l,l+\eta}\beta_i\chi_{i,l+\eta}\beta_{l+\eta} \\
&-8t'\sum_\tau \phi_{l,l+\tau}\beta_i\chi_{i,l+\tau}\beta_{l+\tau}.
\end{aligned}
$$

We also introduce two $N^2 \times N^2$ elements matrices $\widetilde{D}_s$ and $\widetilde{D}_s^z$ to express the spion Green functions. Based on Eq. (7) and (11), we could obtain that

$$
\begin{aligned}
\omega^2\widetilde{D_s} - \widetilde{S}\ \widetilde{D_s} &= \widetilde{C_s} \\
\omega^2\widetilde{D_s^z} - \widetilde{S^z}\ \widetilde{D_s^z} &= \widetilde{C_s^z},
\end{aligned}
\tag{13}
$$

where matrices $\widetilde{S}$, $\widetilde{S^z}$, $\widetilde{C_s}$ and $\widetilde{C_s^z}$ are decided by the density of holon n_i, and the spin correlation functions.

We establish the self-consistent equations based on Eq. (6) and (12) to determine the correlation functions of holon and spinon, and also the vertex correction parameters. Under the periodic boundary conditions, we have performed numerical calculations for 16×16 and 20×20 lattices with different Zn concentrations respectively. Based on the experimental results of BSCCO near optimal doping [1,9], the parameters of t-t′-J model are taken as $t/J = 2.5$ and $t'/t = -0.4$ in our calculations.

Firstly, we study the 20×20 lattice with only one Zn impurity in the optimally doped region ($\delta_h = 0.15$). The spacial distribution of holon density is calculated and our numerical results are shown in figure 1. We find that the holon density closet to the Zn impurity oscillates strongly, and the fluctuation diminishes rapidly away from the Zn impurity. The maximum density is obtained at sites two lattice distances away from the Zn impurity, and is about 15% higher than the minimum density. Our numerical results suggest that doped holes form a local region around the Zn impurity, whose size is about eight lattice cells as shown in figure 1. We also obtain that the magnetic modification introduced by Zn is mainly in the vicinity of Zn impurity. The NN correlation functions near the isolated nonmagnetic impurity in the undoped case have been discussed carefully in Ref. 22. We have found that Zn impurity strongly modifies the spin excitations, especially the magnetic properties of the neighbor Cu. As a result, the AF correlation functions at the bonds closed to the impurities are enhanced. In the optimally doped region, we also obtain that Zn impurity enhances the NN AF correlation functions of spinons close to it. Moreover, The doped holes have the effect to strengthen the AF correlations near the Zn impurity. The ^{63}Cu NMR study of $YBa_2(Cu_{0.99}Zn_{0.01})_3O_{6.7}$ also find that the AF correlations are enhanced, not destroyed, around Zn impurities [13]. Since the quantum fluctuation of spinons close to the nonmagnetic impurity is reduced obviously, we can divided the system into strong AF correlation region and weak AF correlation region. The tendency of doped holes to assemble around the Zn impurity could rationalize anomalous charge localization effect, and the mobility of those holons closed to the Zn impurity could also be reduced. Therefore, a bound state of holon [23] is formed around the Zn impurity. Bound state of impurity in normal state has also been predicted by the self-consistent T matrix approach [18].

We also study the cases with several Zn impurities in the optimally doped regime, and find that the holes play different roles in the strong AF correlation region and the weak AF correlation region. Our numerical results show that the AF correlations of bonds far from the Zn impurity reduces remarkably as hole is added into the systems. On the contrary, the bound state of holon has the effect to enhance the AF correlations around Zn impurity, and helps Zn to introduce local antiferromagnetism around itself. As Zn concentration increases, the CuO_2 plane becomes a inhomogeneous mixture of strong AF correlation regions and weak AF correlation regions. And the doped holes tend to assemble at the strong AF correlation regions.

We show the density of state of holon in cases with several Zn impurities in figure 2. Jung *et al* [24] have examined some samples and prove that Zn is uniformly distributed. In some configurations when Zn is uniformly distributed, our calculation show that due to the strong coupling between impurity and the conduction band, the width of the holon band decreases as Zn concentration increases. We find that the inhomogeneity of the spinon background increases the density of state of holon near the fermi surface, and a resonance peak of impurity states is found to get broader and stronger as Zn concentration increases. Inelastic neutron scattering study for the optimal doped $La_{1.85}Sr_{0.15}Cu_{1-y}Zn_yO_4$ indicates that a new in-gap Zn impuriy state is introduced at low temperature [25]. Nonmagnetic defect structures at the surface has also been found to create localized low-energy excitations in their immediate vicinity in $Bi_2Sr_2CaCu_2O_8$ by performing low-temperature tunneling spectroscopy measurements with a scanning tunneling microscope [4].

Our calculations show that the impurity state can survive above T_c, which is in agreement with the theoretical prediction [18] as well.

To study the effect of the Zn impurity on the spin background around it, we introduce the spin structure factor

$$\mathbf{S}_i(\mathbf{k}) = \sum_j S_i^z S_j^z e^{\mathbf{k}\cdot(\mathbf{i}-\mathbf{j})}. \quad (14)$$

Here i represents Cu site around Zn impurity. Zn impurity is a scatter which has a strong effect on the AF correlation background [26]. As Zn concentration increases, the CuO_2 plane becomes a inhomogeneous mixture of strong AF correlation regions and weak AF correlation regions. In figure 3, the numerical results of the NN Cu sites around Zn impurity are shown for 16×16 lattices with different Zn concentrations. We obtain that, in the pure case and Zn lightly doped case ($\delta_{Zn} \leq 0.01$), the spin excitations are dominated by a magnetic resonance peak located at $Q_{AF} = (\pi, \pi)$. As the Zn concentration increases, this peak decreases and there appear two second-high incommensurate peaks as shown in figure 3, which results from the mixing of $q = (\pi, \pi)$, $q = (\pi, 0)$ and $q = 0$ components in spin excitations introduced by the strong impurity scattering. In Bulut's study of susceptibility of Zn doped high-T_c superconductors, the similar behaviors are also obtained [17]. In addition, we find that the distances of the incommensurate peaks from $q = (\pi, \pi)$ increase with doping, and these peaks become broad and weak in amplitude with the increasing of Zn concentration. Meanwhile, as a result of the increasing of the disorder introduced by the Zn substitution on the Cu sites, the peak at $q = (\pi, \pi)$ decreases gradually as the Zn concentration increases, and disappears when $\delta_{Zn} \geq 0.1$. Thus the result is consistent with experimental results of Zn-doped high-T_c cuprates [11].

In summary, we have studied the interplay between quantum impurities, and collective spinon and holon dynamics in Zn-doped cuprate in the normal state. Within a numerical method based on the Green function theory, the inhomogeneities of holon density distribution and antiferromagnetic correlation background in two-dimensional t-t′-J model with Zn impurities are investigated. We obtain the real space shape of bound state of holon surrounding the nonmagnetic Zn impurity. We also find that the doped holes help Zn to introduce local antiferromagnetism around itself. In the cases with a small amount of Zn impurities, the influence of Zn impurity on the antiferromagnetic correlation background is studied. The appearance of incommensurate peaks in spin structure factor indicates that Zn impurity is a strong scatter center, which has an effect on mixing the $q = (\pi, \pi)$, $q = (\pi, 0)$ and $q = 0$ components in spin excitations.

ACKNOWLEDGMENTS

The authors would like to thank Prof. Feng for helpful discussions. This work was supported by the Grant from Beijing Normal University.

[1] S. H. Pan, E. W. Hudson, K. M. Lang, H. Eisaki, S. Uchida, and J. C. Davis, Nature 403 746 (2000).
[2] Y. Sidis, P. Bourges, H. F. Fong, B. Keimer, L. P. Regnault, J. Bossy, A. Ivanov, B. Hennion, P. Gautier-Picard, G. Collin, D. L. Millius, and I. A. Aksay, Phys. Rev. Lett. **84**, 5900 (2000).
[3] E. W. Hudson, S. H. Pan, A. K. Gupta, K. -W. Ng, and J. C. Davis, Science **285**, 88 (1999).
[4] Ali Yazdani, C. M. Howald, C. P. Lutz, A. Kapitulnik, and D. M. Eigler, Phys. Rev. Lett. **83**, 176 (1999).
[5] A. V. Mahajan, H. Alloul, G. Collin, and J. F. Marucco, Phys. Rev. Lett. **72**, 3100 (1994).
[6] A. Polkovnikov, S. Sachdev, and M. Vojta, Phys. Rev. Lett. **86**, 296 (2001).
[7] A. V. Balatsky, Nature **403** 717 (2000); M. I. Salkola, A. V. Balatsky, and D. J. Scalapino, Phys. Rev. Lett. **77**, 1841 (1996); A. V. Balatsky, M. I. Salkola, and A. Rosengren, Phys. Rev. B **51**, 15547 (1995).
[8] Jian-Xin Zhu, T. K. Lee, C. S. Ting, and Chia-Ren Hu, Phys. Rev. B **61**, 8667 (2000).
[9] H. Tsuchiura1, Y. Tanaka, M. Ogata, and S. Kashiwaya, Phys. Rev. Lett. **84**, 3165 (2000); J. Phys. Soc. Jpn. **68**, 2510 (1999).
[10] T. Xiang, Y. H. Su, C. Panagopoulos, Z. B. Su, and L. Yu, Phys. Rev. B **66**, 174504 (2002).
[11] H. Alloul, P. Mendels, H. Casalta, J. F. Marucco, and J. Arabski, Phys. Rev. Lett **67**, 3140 (1991).
[12] J. Bobroff, H. Alloul, Y. Yoshinari, A. Keren, P. Mendels, N. Blanchard, G. Collin, and J.-F. Marucco, Phys. Rev. Lett. **79**, 2117 (1997); J. Bobroff, W. A. MacFarlane, H. Alloul, P. Mendels, N. Blanchard, G. Collin, and J.-F. Marucco, Phys. Rev. Lett. **83**, 4381 (1999).
[13] M.-H. Julien, T. Fehér, M. Horvatic, C. Berthier, O. N. Bakharev, P. Ségransan, G. Collin, and J.-F. Marucco, Phys. Rev. Lett. **84**, 3422 (2000).
[14] W. A. MacFarlane, J. Bobroff, H. Alloul, P. Mendels, N. Blanchard, G. Collin, and J.-F. Marucco, Phys. Rev. Lett. **85**, 1108 (2000).
[15] H. Yamagata, H. Miyamoto, K. Nakamura, M. Matsumura, and Y. Itoh, cond-mat/0304477.
[16] N. Nagaosa and P. A. Lee, Phys. Rev. Lett. **79**, 3755 (1997).
[17] N. Bulut, Phys. Rev. B **61**, 9051 (2000).
[18] H. V. Kruis, I. Martin, and A. V. Balatsky, Phys. Rev. B **64**, 054501 (2001).
[19] J. L. Tallon, C. Bernhard, G. V. M. Williams, and J. W. Loram, Phys. Rev. Lett. **79**, 5294 (1997); J. L. Tallon, Phys. Rev. B **58**, 5956 (1998).
[20] B. Chattopadhyay, B. Bandyopadhyay, A. Poddar, P.

Mandal, A. N. Das, and B. Ghosh, Physica C **331**, 38 (2000).
[21] Shiping Feng, Z. B. Su, and L. Yu, Phys. Rev. B **49**, 2368 (1994); Mod. Phys. Lett. B **7**, 1013 (1993); Shiping Feng and Yun Song, Phys. Rev. B **55** 642 (1997).
[22] Yun Song, H. Q. Lin and Jue-Lian Shen, Phys. Rev. B **58**, 9166 (1998); Yun Song, H. Q. Lin and A. W. Sandvik, J. Phys.: Condens. Matter **12**, 5275 (2000).
[23] D. Poilblanc, D. J. Scalapino, and W. Hanke, Phys. Rev. Lett. **72**, 884 (1994); W. Ziegler, D. Poilblanc, R. Preuss, W. Hanke, and D. J. Scalapino, Phys. Rev. B **53**, 8704 (1996).
[24] C. U. Jung, J. Y. Kim, Min-Seok Park, Mun-Seog Kim, Heon-Jung Kim, S. Y. Lee, and Sung-Ik Lee, Phys. Rev. B **65**, 172501 (2002).
[25] H. Kimura, M. Kofu, Y. Matsumoto, and K. Hirota, cond-mat/0209428.
[26] O. P. Vajk, P. K. Mang, M. Greven, P. M. Gehring, and J. W. Lynn, Science, 295, 1691 (2002).

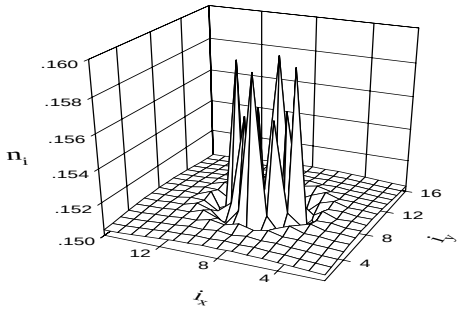


FIG. 1. The distribution of holon density in a 20×20 lattice with only one Zn impurity.

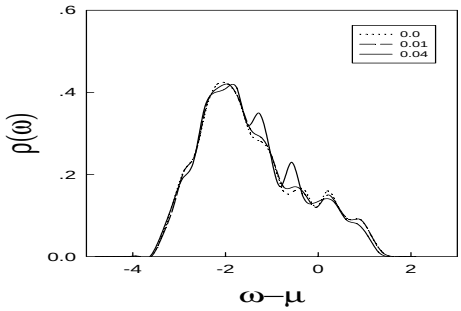


FIG. 2. The density of state of holon at δ_{Zn}=0.0 (dotted line), 0.01(dashed line), and 0.04 (solid line).

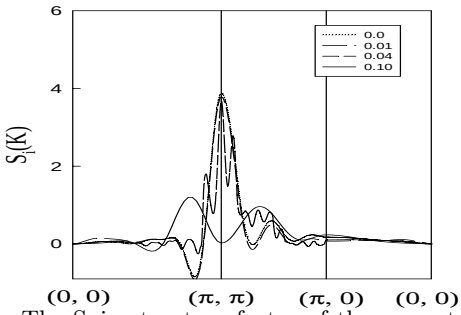


FIG. 3. The Spin structure factor of the nearest neighbor Cu sites around Zn impurity for 16×16 lattices with different Zn concentrations.